# Linear Modal Analysis of Doubly-Fed Induction Generator (DFIG) Torsional Interaction: Effect of DFIG Controllers and System Parameters

*Ali ZIAEI*[1], *Reza GHAZI*[1], *Roohalamin ZEINALI DAVARANI*[2]

[1]Department of Electrical Engineering, Faculty of Engineering, Ferdowsi University of Mashhad, Razavi Khorasan Province, Mashhad, Iran
[2]Department of Electrical Engineering, Faculty of Electrical and Computer Engineering, Graduate University of Advanced Technology, Kerman Province, Iran

ali.ziayi@alumni.um.ac.ir, r.ghazi@um.ac.ir, r.zeinali@kgut.ac.ir

DOI: 10.15598/aeee.v16i4.2265

***Abstract.*** *Clean energy sources like wind energy have received great attention due to growing demand for electrical energy and increase of environmental pollution. The Doubly Fed Induction Generators (DFIGs) are also in common use due to their ability to control the reactive power with no need for capacitor banks. Existence of active and reactive power controllers in DFIG may provide the possibility of adverse interaction with torsional modes of the turbine-generator set. Because of the importance of this phenomenon, in this paper, the interaction of DFIG controllers with other components of the wind turbine-generator, especially torsional modes, has been studied. As the variable speed wind turbine is used, the effects of rotor speed variation on the torsional interaction with the active and reactive power controllers have been investigated. Moreover, the effects of variation of other parameters such as local load, and mechanical and electrical parameters of DFIG on the torsional interaction have been studied. In order to study and analyze this phenomenon, the linear modal analysis is used. The obtained results demonstrate the effects of parameters in possible occurrence of interaction between the DFIG controllers and the DFIG turbine generator set. In addition, the obtained analytical results are verified via time domain simulation.*

## Keywords

***Doubly Fed Induction Generator (DFIG), linear modal analysis, system modes, torsional modes, Wind Turbine (WT).***

## 1. Introduction

Installation of wind power plants is rapidly increasing due to their environmental benefits and the limitation of fossil fuel resources. The variable speed wind turbines have supplanted the fixed speed ones as offering the improved power quality. In addition, the Doubly Fed Induction Generators (DFIG, s) are also in common use due to their ability to control the reactive power with no need for capacitor banks. Nowadays, the operation of wind turbines with higher levels of power is further increasing. With regard to their unique characteristics such as high turbine inertia compared with the low inertia of generator and low shaft stiffness coefficient, the multi-mass model is used for the wind turbine-generator shaft [1] and [2]. The modes associated with these masses are called torsional modes, and the corresponding oscillations are called torsional oscillations. The interaction of power system components with the turbine generator set may result in torsional modes excitation leading to an increase in the amplitudes of torsional oscillations experienced by the shaft. The possible occurrence of interaction phenomenon and its severity can be emanated from control and/or system parameters. The resulting adverse effects may jeopardize the system dynamic performance and its stability. Therefore, the interaction between the system modes and the torsional modes must be studied carefully.

In literature, the torsional interaction commonly has reported in the following four situations: Sub-Synchronous Resonance (SSR) in a series compensated transmission line [3], [4], [5], [6] and [7], interaction with the generator excitation control [8], interaction with speed governors [9] and torsional interaction with system controllers [10], [11] and [12]. In addition, in [13], [14], [15] and [16], the effects of system parameters on the damping of torsional modes are investigated. In [13], [14] and [15], by using time domain simulation and linear modal analysis, the interaction between the wind turbine-generator set and the system modes referred to as inter-area and local modes has been studied. The outcome results show that when the capacity of wind farm increases, the interaction between wind turbine-generator set and other system components increases. In Ref. [16], it is shown that the probability of torsional interaction in hydro turbine-generator having low inertia with respect to the generator inertia is very high. In [17], by using the linear modal analysis, the torsional interaction of a wind farm connected to a series compensated network is studied. This reference shows that the frequency and damping ratio of SSR mode are reduced with the increase of the compensation level due to the phenomenon known as Induction Generator Effect (IGE). Reference [18] presents a new technique to damp sub-synchronous oscillations in a series compensated system. The proposed technique uses the voltage at the point of common coupling in cascaded compensators to magnify the positive resistance without using generator or turbine speed and/or torque perturbations. In Ref. [19], a proportional control loop is added to the torque control to reduce the influence of the inertia moment in the wind turbines, so as to improve its dynamic performance. Reference [20] presents a damping control to mitigate sub-synchronous interactions in Doubly-Fed Induction Generator (DFIG) wind turbines connected to series-compensated lines. The obtained results show that the supplementary control is able to properly damp the sub-synchronous oscillations of DFIG wind turbines and reduce the risk of wind generation tripping. Reference [21] uses an energy storage system for improving the power system stability with grid-connected distributed generation. Reference [22] has briefly investigated the interaction of the DFIG controllers with torsional modes of the wind turbine shaft.

In previous studies, the interactions of DFIG controllers with other system components are not thoroughly investigated. The interaction of DFIG controllers with other system components increases the amplitude of the system electrical and mechanical oscillations and in the worst case, leads to instability of the power system. Especially, if there is an interaction between DFIG controllers and turbine-generator shaft, the amplitude of torsional oscillations is increased and led to reduction of the lifetime of the turbine-generator. In the worst case, if the interaction leads to instability of torsional modes, intensive torque experienced by the turbine-generator shaft. So, in tuning of DFIG controllers, the interaction of controllers with other system components should be studied carefully. So, in the present paper, attempts are made to tackle the problem further considering various parameters and identify the most effective ones. These parameters include: the mechanical and electrical parameters of DFIG and its controllers, the rotor speeds and local loads. Based on the results of this study, the proper preventive actions can be taken to mitigate the adverse effects of interaction.

To do this study, first, the differential equations governing the dynamic behaviour of the studied system are provided. It should be noted that the multi-mass model is used for the turbine-generator set. Then, by using the linear modal analysis, the interaction phenomenon is investigated regarding the intended parameters. From the linearized system, the eigenvalues are obtained. Based on the linear analysis theory if all the eigenvalues have positive damping coefficient, the system is stable and if one of the eigenvalues has negative damping coefficient, the system is unstable. To investigate the interaction between DFIG controllers and other system components through Eigenvalue analysis, the MATLAB software is used. In addition, the obtained analytical results are validated by simulations using MATLAB/Simulink.

The paper is organized as follows. In Sec. 2. , the modelling of wind turbine-generator components is presented. The linear modal analysis method is described in Sec. 3. In Sec. 4. , by using this method, the interaction between the DFIG controllers and other parts of the wind turbine-generator is studied. In addition, the effects of the rotor speed variations, local load variations, and electrical and mechanical parameters of the wind turbine-generator set on the torsional modes are given in this section. Finally, Sec. 5. concludes the paper.

# 2. Modelling of Wind Turbine-Generator Components

In this section, the model of different components of the wind turbine-generator set is provided.

## 2.1. Wind Turbine

The available wind turbines are classified into four main categories. Both types A and B are based on the induction generator where type A provides fixed speed operation and type B also has a limited range of operation at the variable speed. The main disadvantage of these configurations is the fluctuating power transmitted to the grid resulting from wind speed variations. Types C and D are based on DFIG and PMSG (Permanent Magnet Synchronous Generator) which provide the variable-speed operation under various control schemes [23] and [24]. The output power with less fluctuations and the optimal extraction of power from wind are their main advantages. As type C is the most commonly used in wind farm projects [23], this type of wind turbine is used in this paper.

The mechanical power extracted from a wind turbine can be estimated by:

$$P_t = \frac{1}{2}\rho A v_\omega^3 C_p, \tag{1}$$

where $\rho$ is the air density (kg·m$^{-3}$), $A$ is the wind turbine swept area (m$^2$), $v_\omega$ is the wind speed (m·s$^{-1}$) and $C_p$ is the power coefficient. $C_p$ is the function of pitch angle ($\beta$), the method of blades design and the tip speed ratio ($\lambda$) and is calculated as follows:

$$C_p(\lambda,\beta) = 0.5176\left(\frac{116}{\lambda_i} - 0.4\beta - 5\right)e^{\frac{21}{\lambda_i}} + 0.0068\lambda,$$

$$\lambda_i\left(\frac{1}{\lambda + 0.08\beta} - \frac{0.035}{\beta^3+1}\right)^{-1}, \quad \lambda = \frac{\omega_{tur}R}{V_\omega}, \tag{2}$$

where $\omega_{tur}$ equals to the angular velocity of blades, and $R$ is the rotor radius.

The wind turbine includes blades and hub, low-speed shaft, gearbox, high-speed shaft and generator. The three mass model is used to represent the wind turbine-generator shaft as shown in Fig. 1. With this classification, six state variables for the mechanical part of the wind turbine are considered as follows:

$$\omega_{gen},\ \omega_{hub},\ \omega_{blade},\ \delta_{gen},\ \delta_{hub},\ \delta_{blade}. \tag{3}$$

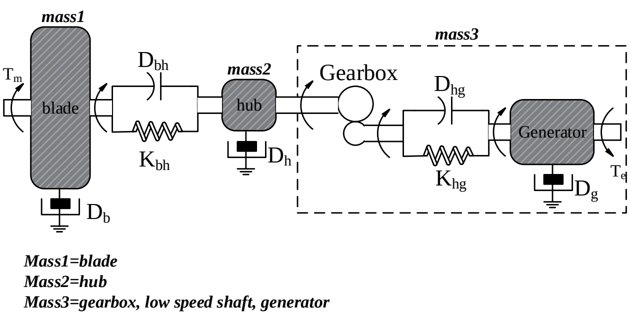


**Fig. 1:** The components of three mass model for wind turbine.

The equations related to the wind turbine-generator shaft are given as below:

$$\frac{d\omega_{blade}}{dt} = \frac{1}{2H_{blade}}\begin{bmatrix} T_m - K_{bh}(\delta_{blade} - \delta_{hub}) \\ -D_{bh}(\omega_{blade} - \omega_{hub}) \\ -D_b(\omega_{blade} - \omega_{ref}) \end{bmatrix}, \tag{4}$$

$$\frac{d\delta_{blade}}{dt} = \omega_s(\omega_{blade} - \omega_{ref});\ \omega_{ref} = (1-s)\omega_s, \tag{5}$$

$$\frac{d\omega_{blade}}{dt} = \frac{1}{2H_{blade}}\begin{bmatrix} -K_{bh}(\delta_{hub} - \delta_{blade}) \\ -K'_{hg}K_{gear}(K_{gear}\delta_{hub} - \delta_{gen}) \\ -D_{hg}K_{gear}(K_{gear}\omega_{hub} - \omega_{gen}) \\ -D_{bh}(\omega_{hub} - \omega_{blade}) \\ -d_h(\omega_{hub} - \omega_{ref}) \end{bmatrix}, \tag{6}$$

$$\frac{d\delta_{hub}}{dt} = \omega_s(\omega_{hub} - \omega_{ref});\ \omega_{ref} = (1-s)\omega_s, \tag{7}$$

$$\frac{d\omega_{gen}}{dt} = \frac{1}{2H_{gen}}\begin{bmatrix} -T_e - K_{hg}(\delta_{gen} - K_{gear}\delta_{hub}) \\ -D_{hg}(\omega_{gen} - K_{gear}\omega_{hub}) \\ -D_g(\omega_{gen} - \omega_{ref}) \end{bmatrix}, \tag{8}$$

$$\frac{d\delta_{gen}}{dt} = \omega_s(\omega_{gen} - \omega_{ref});\ \omega_{ref} = (1-s)\omega_s, \tag{9}$$

where $\omega_{blade}$, $\omega_{hub}$ and $\omega_{gen}$ are the angular speed of the blades, hub and generator, respectively. Moreover, $H_{blade}$, $H_{hub}$ and $H_{gen}$ are the inertia constants, $\delta_{blade}$, $\delta_{hub}$ and $\delta_{gen}$ are the rotational displacement, $D_b$, $D_h$ and $D_g$ are damping coefficients of the blades, hub and generator, respectively. $D_{bh}$ is damping coefficient of the shaft between blades and hub, $D_{hg}$ is damping coefficient of the shaft between hub and generator, $K_{bh}$ is the stiffness coefficient of the shaft between blades and hub and $K_{hg}$ is the stiffness coefficient of the shaft between hub and generator. $K_{gear}$ is the transformation ratio of the gearbox, $T_e$ is the electrical torque, and $T_m$ is the aerodynamic torque provided by the wind.

## 2.2. Doubly Fed Induction Generator (DFIG)

Figure 2 shows a variable speed wind turbine connected to a DFIG. In this figure, the rotor is equipped with two converters and a DC link capacitor.

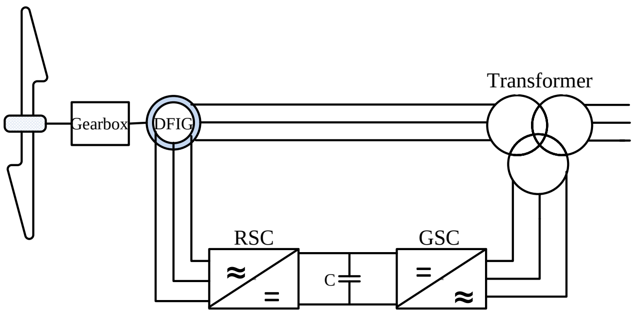


**Fig. 2:** Wind turbine equipped with DFIG.

For the dynamic equations of the DFIG, the state variables for $q$ and $d$ components of the stator and rotor currents and its controllers are considered as follows:

$$I_{qs},\ I_{ds},\ I_{qr},\ I_{dr},\ x_1,\ x_2,\ x_3,\ x_4. \tag{10}$$

The electrical equations of DFIG are given by:

$$\frac{dI_{qs}}{dt} = \frac{\omega_b}{X'_s}\begin{pmatrix} -V_{qs} + \frac{X_m}{X_r}V_{qr} - R_sI_{qs} - \\ \frac{X_m}{T'o\omega_b}I_{qr} + AI_{ds} + \frac{\omega_r X_m}{\omega_b}I_{dr} \end{pmatrix}, \tag{11}$$

$$\frac{\mathrm{d}I_{ds}}{\mathrm{d}t} = \frac{-\omega_b}{X'_s} \begin{pmatrix} -V_{ds} - \dfrac{X_m}{X_r}V_{dr} + R_s I_{ds} + \\ \dfrac{X_m}{T'o\omega_b}I_{dr} + AI_{qs} + \dfrac{\omega_r X_m}{\omega_b}I_{qr} \end{pmatrix}, \quad (12)$$

$$\frac{\mathrm{d}I_{qr}}{\mathrm{d}t} = \frac{\omega_b}{X_m} \begin{pmatrix} BV_{qs} + R_s B I_{qs} + B\left(\dfrac{\omega'_r X_s}{\omega_b}\right) I_{ds} + \\ CX_m I_{dr} - \dfrac{X_s X_m}{X'_s T' o\omega_b} I_{qr} + \dfrac{X_s X_m}{X'_s X_r} V_{qr} \end{pmatrix}, \quad (13)$$

$$\frac{\mathrm{d}I_{dr}}{\mathrm{d}t} = \frac{\omega_b}{X_m} \begin{pmatrix} BV_{ds} + R_s B I_{ds} - B\left(\dfrac{\omega_r X_s}{\omega_b}\right) I_{qs} - \\ CX_m I_{qr} - \dfrac{X_s X_m}{X'_s T' o\omega_b} I_{dr} + \dfrac{X_s X_m}{X'_s X_r} V_{dr} \end{pmatrix}. \quad (14)$$

Such that,

$$\begin{aligned} T'_o &= \frac{X_r}{\omega_b R_r}; \omega_b = \omega_s;\ \omega_r = \omega_{gen}; \\ X'_s &= X_s - \frac{X_m^2}{X_r};\ A = \left(\frac{\omega_r - \omega}{\omega_b} S'_s - \frac{\omega_r}{\omega_b} X_s\right); \\ B &= \left(\frac{X'_s - X_s}{X'_s}\right);\ C' \left(\frac{\omega_r X_s}{\omega_b X'_s} - \frac{\omega}{\omega_b}\right), \end{aligned} \quad (15)$$

where $V$, $I$, $R$ and $X$ correspond to voltages (p.u.), currents (p.u.), resistances (p.u.) and reactances (p.u), respectively. Also, $X_m$ is the mutual reactance between stator and rotor, $X_s = X_{ls} + X_m$ is the stator reactance and $X_r = X_{lr} + X_m$ is the rotor reactance. $X_{ls}$ and $X_{lr}$ are the stator and rotor leakage reactance, respectively.

The electrical torque $T_e$ in the Eq. (8) is given by:

$$T_e = X_m (I_{qs} I_{dr} - I_{ds} I_{qr}). \quad (16)$$

The block diagram of the DFIG active and reactive power controllers is shown in Fig. 3. The method of design and selection of controllers parameters are described in [23].

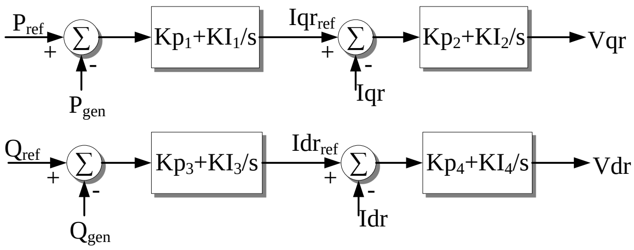


**Fig. 3:** Active and reactive power controllers of DFIG.

The differential equations of the active and reactive controllers are obtained as:

$$\frac{\mathrm{d}x_1}{\mathrm{d}t} = k_{I1}(P_{ref} - P_{gen}), \quad (17)$$

$$\frac{\mathrm{d}x_2}{\mathrm{d}t} = k_{I2}(k_{p1}(P_{ref} - P_{gen}) + x_1 - I_{qr}), \quad (18)$$

$$\frac{\mathrm{d}x_3}{\mathrm{d}t} = k_{I3}(Q_{ref} - Q_{gen}), \quad (19)$$

$$\frac{\mathrm{d}x_4}{\mathrm{d}t} = k_{I4}(k_{p3}(Q_{ref} - Q_{gen}) + x_3 - I_{dr}). \quad (20)$$

In Ref. [24], it is shown that the dynamics of the Grid Side Converter (GSC) are much faster than that of the Rotor Side Converter (RSC), and the controller also has a weak coupling with other state variables resulting from participation coefficients analysis. Therefore, the grid side converter dynamic is neglected in the modelling of the wind turbine-generator set. In this study, the $\pi$ model is used for the transmission line.

## 3. Linear Modal Analysis

Linear modal analysis is a well-known method to study the interaction phenomenon in the power system. To investigate the interaction problem, the dynamic equations of power system components to be provided first. Suppose that Eq. (21) represents the dynamic equations of a power system.

$$\begin{aligned} \dot{x}_1 &= F_1(x_1, \ldots, x_n), \\ \dot{x}_2 &= F_2(x_1, \ldots, x_n), \\ &\vdots \\ \dot{x}_n &= F_n(x_1, \ldots, x_n), \end{aligned} \quad (21)$$

where $x_i$ denotes $i$-state variable and $\dot{x}_i$ denotes the state equation associated with it. The relationship between the state variables $\dot{x}_i$ and $x_1 - x_n$ is shown as a function $F_i$. Since $F_i s$ are general nonlinear functions, so for the linear modal analysis, the first-order Taylor expansion of functions is obtained around the stable equilibrium point.

$$X_i = A_i X, \quad (22)$$

where $A_i$ is the $i^{\text{th}}$ row of the Jacobian matrix and is calculated by:

$$\mathbf{A} = \frac{\partial F}{\partial X}. \quad (23)$$

To investigate the interaction of the wind turbine, the Eigenvalues of the Jacobian matrix $\mathbf{A}$ are obtained, and by using the participation matrix, the Eigenvalue associated with each component are identified. Finally, via Eigenvalue analysis, the effects of different conditions of controllers on the damping of considered Eigenvalues are studied and discussed [25].

## 4. Interaction of DFIG Active and Reactive Power Controllers with Wind Turbine Components

The studied system is a 9 MW wind farm comprising six 1.5 MW wind turbines connected to a 25 kV distribution system which injects power to the infinite bus via a transmission line. The power curve of considered 1.5 MW wind turbine is shown in Fig. 4. It is supposed that the wind speed is higher than 12 m·s$^{-1}$. As shown in Fig. 4, for wind speed higher than 12 m·s$^{-1}$, the nominal power 1.5 MW can be extracted from DFIG.

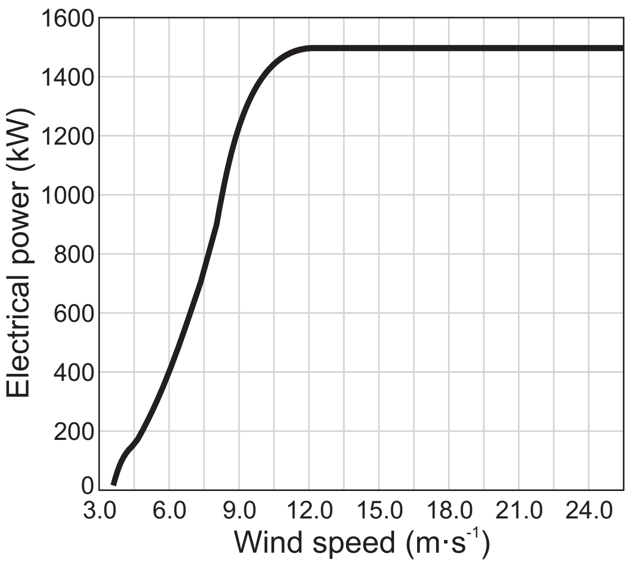


**Fig. 4:** Power curve of considered 1.5 MW wind turbine.

Model Reduction is often applied to obtain a lower order model in the control design stage [20]. So, wind farm is modelled with a wind turbine-generator based on DFIG, and its equivalent model is obtained using the aggregated technique [26].

The block diagram of the test system is shown in Fig. 5. The test system parameters are listed in the App. A.

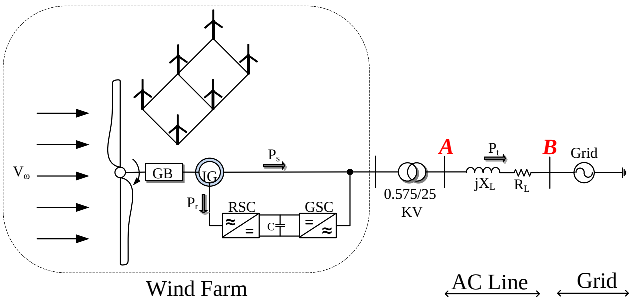


**Fig. 5:** Single line diagram of the test system.

The Eigenvalue analysis of the test system is carried out, and the results are shown in Tab. 1. As seen from the Tab. 1, the frequency of the system mode is 0.28 Hz and the frequencies of torsional modes are 1.014 Hz and 5.344 Hz.

Then, regarding the feasible range of parameters of the active and reactive power controllers of DFIG, their effects on the damping of other system modes are examined. It is obvious that in such cases other parameters of controllers are kept constant while the system operating points owing to system changes are recalculated. For the sake of simplicity, a multiplication *factor* is considered as below:

$$\begin{aligned} K_P^{new} &= factor \times K_P^{base}, \\ K_I^{new} &= factor \times K_I^{base}. \end{aligned} \tag{24}$$

The interaction of these controllers is reported in the following subsections. In what follows, the above *factor* has been changed between 0.2 and 4.

## 4.1. Active Power Controller

As shown in Fig. 3, the active power controller of DFIG includes two sub-controllers ($K_{P1} - K_{I1}$, $K_{P2} - K_{I2}$). The effect of the external sub-controller ($K_{P1} - K_{I1}$) is studied first. By increasing the parameter factor from 0.2 to 4, the Eigenvalues of the test system are obtained and the damping ratio of system modes is shown in Fig. 6. The results for torsional modes are individually provided in Fig. 7.

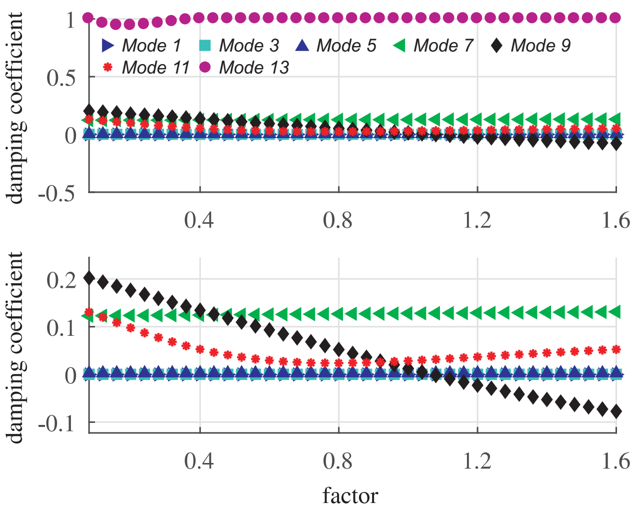


**Fig. 6:** Effect of increasing the parameters $K_{P1}$ and $K_{I1}$ on the system damping modes.

As seen in Fig. 6, by increasing the gains of the external active power controller ($K_{P1}$ and $K_{I1}$), the damping of some modes such as mode 9 is noticeably decreased. For instance, when the parameter factor is greater than 2.7, the mode 9 becomes unstable. As seen in Tab. 1, mode 9 is an electrical mode, and its instability will result in the severe increase of electrical oscillations. In addition, Fig. 7 shows that increasing the gains ($K_{P1} - K_{I1}$) leads to slight decrease of torsional modes damping. The damping of torsional mode 1 always decreases as the parameters increase. Also,

**Tab. 1:** Eigenvalues analysis of the test system.

| Mode | Eigenvalue | Damping | Frequency (Hz) | Source |
|---|---|---|---|---|
| 1,2 | $-0.002\pm$j33.5764 | $5.8997 \cdot 10^{-5}$ | 5.344 | $\omega_{gen}$, $\omega_{hub}$, $\omega_{gen}$, $\omega_{hub}$ |
| 3,4 | $-0.0025\pm$j6.3709 | $3.9931 \cdot 10^{-4}$ | 1.014 | $\omega_{gen}$, $\omega_{hub}$, $\omega_{blade}$, $\omega_{gen}$, $\omega_{hub}$, $\omega_{blade}$ |
| 5,6 | $-0.0044\pm$j1.7545 | 0.0025 | 0.2792 | $\omega_{blade}$, $\delta_{blade}$ |
| 7,8 | $-45.18\pm$j359.94 | 0.1245 | 57.28 | $I_{qs}$, $I_{ds}$, $I_{qr}$, $I_{dr}$ |
| 9,10 | $-1.9645\pm$j14.4766 | 0.1345 | 2.3040 | $I_{qs}$, $I_{ds}$, $I_{qr}$, $I_{dr}$ |
| 11,12 | $-0.517\pm$j9.8044 | 0.0527 | 1.5604 | $I_{qs}$, $I_{ds}$, $I_{qr}$, $I_{dr}$, $x_2$, $x_4$ |
| 13 | $-2.6583$ | 1 | 0 | $x_1$, $x_3$ |
| 14 | $-3.2717$ | 1 | 0 | $x_1$, $x_3$ |

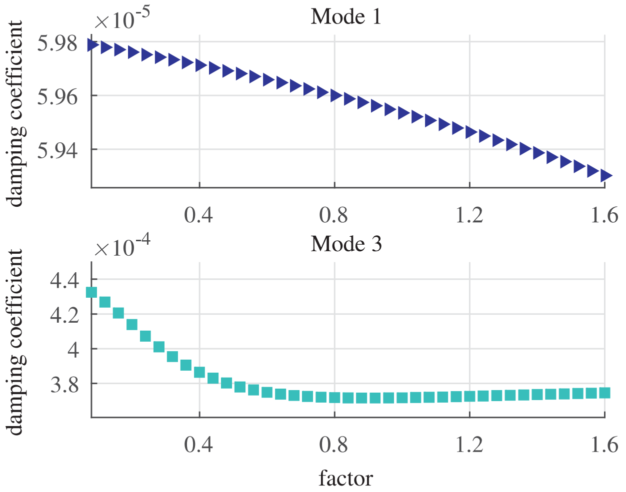


**Fig. 7:** Effect of increasing the parameters $K_{P1}$ and $K_{I1}$ on the damping of torsional modes.

the damping of torsional mode 3 initially decreases and then slightly increases.

To verify the analytical results, the time response of the test system for different values of $K_{P1}$ and $K_{I1}$ is obtained, and the results are shown in Fig. 8. The simulation is done for increasing wind power generation (Pgen) from 0.8 pu to 1 pu.

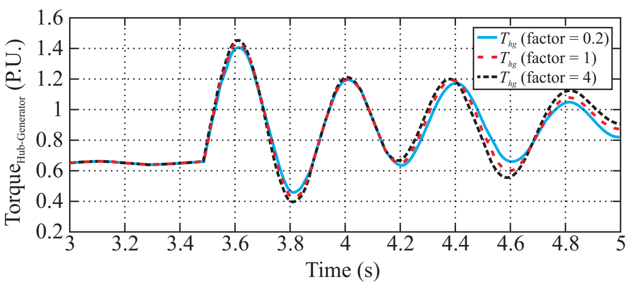


**Fig. 8:** Oscillation torque imposed on shaft between hub and generator for different values of active power controller gains($K_{P1} - K_{I1}$).

As seen in Fig. 8, by increasing the external active power controller gains, the amplitude of torsional torque imposed on the shaft of the wind turbine generator will be slightly increased, which verifies the analytical results shown in Fig. 7.

Similar to the active power controller gains ($K_{P1} - K_{I1}$), the effects of other active power controller gains ($K_{P2} - K_{I2}$) on the system mode damping are studied and the results are shown in Fig. 9 and Fig. 10. The results show that unlike those results, increasing the gains leads to increasing the damping of system mode, which is obvious in modes 7, 9 and 11. Figure 9 shows that by selecting lower values for controller parameters $K_{P2}$ and $K_{I2}$, the electrical mode 11 becomes unstable and leads to instability of system electrical oscillations.

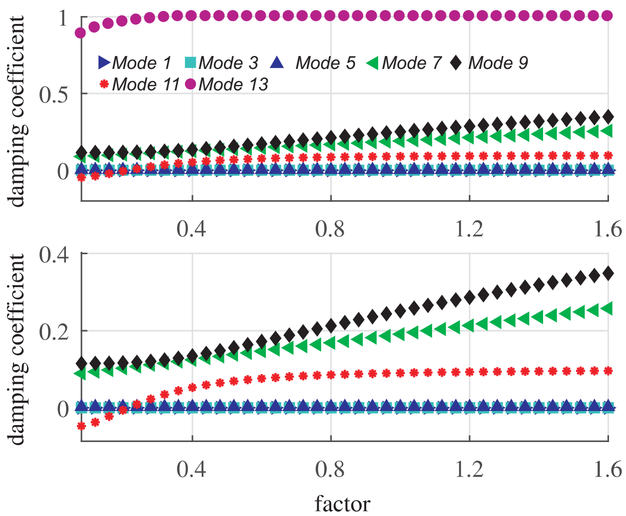


**Fig. 9:** Effect of increasing the parameters $K_{P2}$ and $K_{I2}$ on the system damping modes.

In addition, as seen in Fig. 10, in this case, the damping of torsional mode 1 is noticeably increased. Furthermore, for lower values of $K_{P2}$ and $K_{I2}$, the damping coefficient of torsional mode 3 is negative and leads to instability of the power system. The torsional torque imposed on the shaft for different values of $K_{P2}$ and $K_{I2}$ is obtained, and the results are shown in Fig. 11. As seen by selecting lower values for $K_{P2}$ and $K_{I2}$, the amplitude of torsional torque is noticeably increased and leads to severe damage to the shaft. Therefore, the simulation results validate the analytical results obtained by linear analysis.

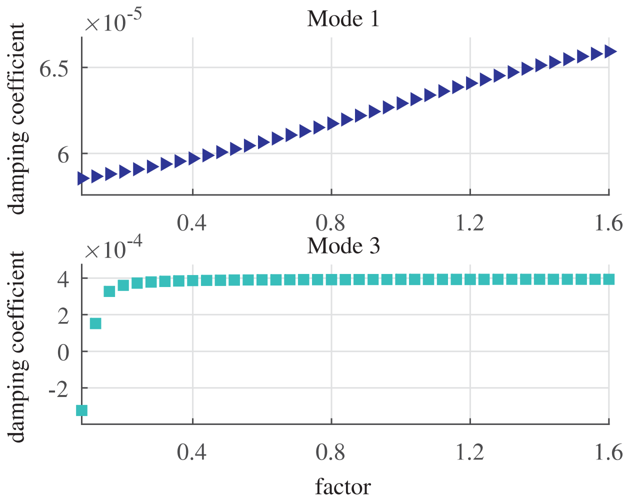


**Fig. 10:** Effect of increasing the parameters $K_{P2}$ and $K_{I2}$ on the damping of torsional modes.

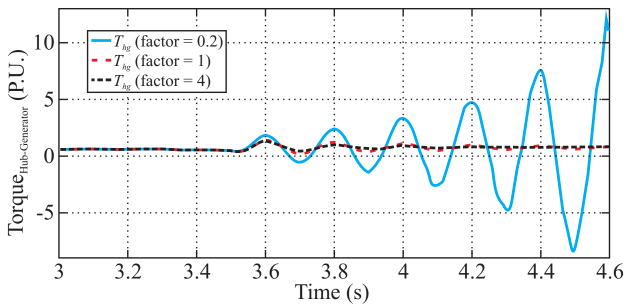


**Fig. 11:** Oscillation torque imposed on shaft between hub and generator for different values of controller parameters ($K_{P2} - K_{I2}$).

## 4.2. Reactive Power Controller

Similar to the previous section, the effect of the reactive power controller on the system modes damping study and the results are shown in Fig. 12 to Fig. 17.

As seen in Fig. 12, the modes 9 and 11 are experiencing the most effect from reactive power controller parameters $K_{P3}$ and $K_{I3}$ such that for higher values of these parameters, mode 9 becomes unstable leading to instability of system electrical oscillations. In addition, as seen in Fig. 13, by increasing the values of reactive controller parameters $K_{P3}$ and $K_{I3}$, the damping coefficient of torsional mode 1 and 3 slightly decreases and increases, respectively.

The torsional torque imposed on the shaft for different values of $K_{P3}$ and $K_{I3}$ is shown in Fig. 14. As seen in Fig. 14, by increasing these controller gains, the amplitude of torsional torque imposed on the shaft is increased by a very small value.

As seen in Fig. 15, reactive power controller parameters ($K_{P4}$ and $K_{I4}$) affect the modes 7, 9 and 11. Figure 15 shows that for lower values of $K_{P4}$ and $K_{I4}$,

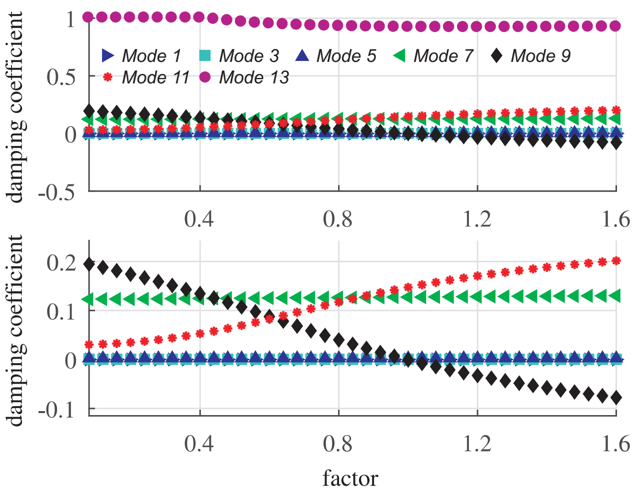


**Fig. 12:** Effect of increasing the parameters $K_{P3}$ and $K_{I3}$ on the system damping modes.

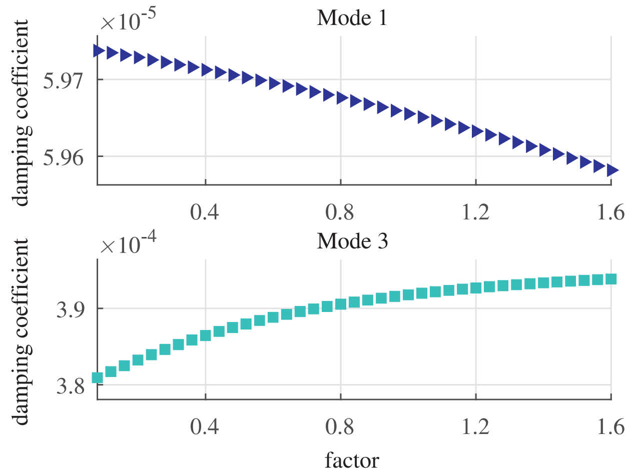


**Fig. 13:** Effect of increasing the parameters $K_{P3}$ and $K_{I3}$ on the damping of torsional modes.

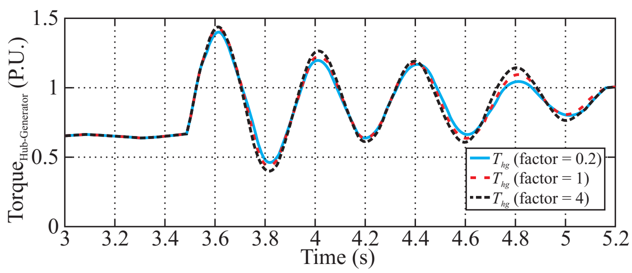


**Fig. 14:** Oscillation torque imposed on shaft between hub and generator for different values of controller gains ($K_{P3} - K_{I3}$).

mode 11 becomes unstable leading to instability of system electrical oscillations. In addition, Fig. 16 shows that by increasing the values of reactive controller parameters $K_{P4}$ and $K_{I4}$, the damping coefficient of torsional mode 3 decreases.

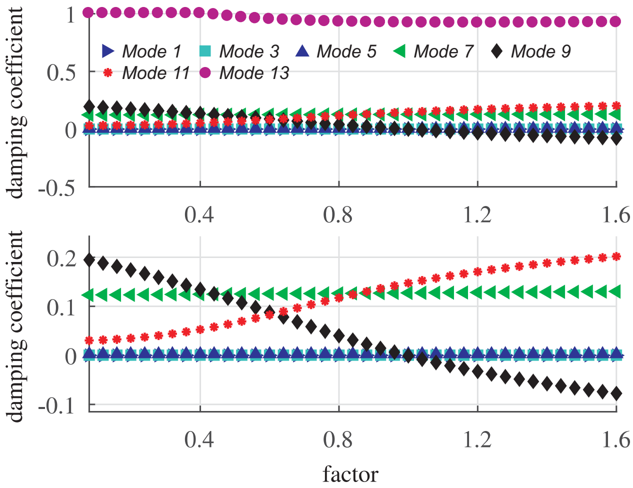


**Fig. 15:** Effect of increasing parameters $K_{P4}$ and $K_{I4}$ on the system damping modes.

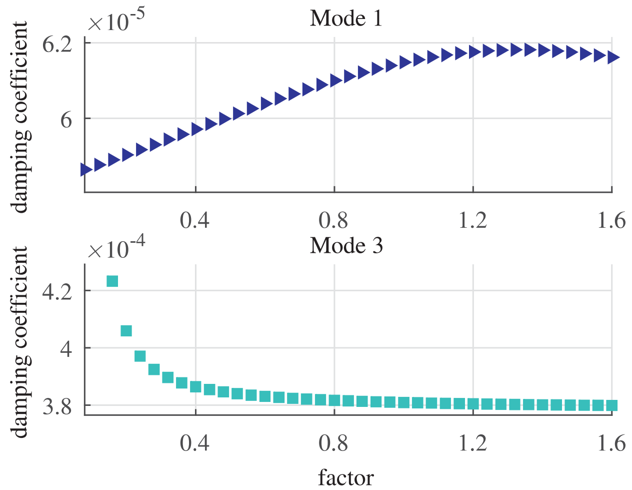


**Fig. 16:** Effect of increasing the parameters $K_{P4}$ and $K_{I4}$ on the damping of torsional modes.

Figure 17 shows that by increasing the internal reactive power controller gains, the amplitude of torsional torque imposed on the shaft is decreased.

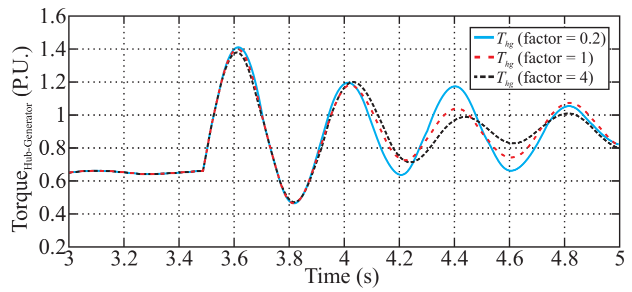


**Fig. 17:** Oscillation torque imposed on shaft between hub and generator for different values controller gains ($K_{P4} - K_{I4}$).

Comparing the results from active and reactive power controllers shows that the effect of the internal active power controller ($K_{P2} - K_{I2}$) on the system modes damping, is more pronounced than other controllers.

For further study of torsional interaction with DFIG controllers, the active and reactive power controllers parameters ($K_P$ and $K_I$) are changed independently, and the results are shown in Tab. 2. As seen in this table, the DFIG controller parameters can affect the torsional modes in different ways.

## 4.3. Effect of Rotor Speed, Local Load, and Wind Turbine-Generator Electrical and Mechanical Parameters on the Damping of Torsional Modes

In this section, the effect of some important factors of the system, such as rotor speed, local load, and electrical and mechanical parameters, on the torsional interaction with active and reactive power controllers is studied. For this purpose, for different values of these factors, the effect of active and reactive power controllers on the damping of torsional modes is investigated. Since the similar results are obtained for both torsional mode 1 and 3, only the results related to torsional mode 1 are shown.

### 1) Rotor Speed ($\omega_r$)

For different values of rotor speeds ($270 - -470$ rad·s$^{-1}$), the effect of active and reactive power controllers on the damping of torsional mode 1 is studied, and the results are shown in Fig. 18. As seen in this figure, the torsional interaction of both parts of the active power controller ($K_{P1}$ and $K_{I1}$, $K_{P2}$ and $K_{I2}$) is affected by the DFIG rotor speed. The results show that, at the lower rotor speed, by increasing the gains of active power external controller ($K_{P1}$ and $K_{I1}$), the damping of torsional mode 1 is decreased. While that at the higher rotor speed by increasing the gains $K_{P1}$ and $K_{I1}$, the damping of torsional mode 1 is increased. In addition, the results show that, at the lower rotor speed, by increasing the gains of the active power internal controller ($K_{P2}$ and $K_{I2}$), first the damping of torsional mode is increased, and then decreased. Whereas at the higher rotor speed, by increasing the gains $K_{P2}$ and $K_{I2}$, the damping of torsional mode is strictly increased.

**Tab. 2:** The results of independent change in the proportional and integral parameters of the active and reactive power controllers.

| Torsional Modes | Active power external controller | | Active power internal controller | | Reactive power external controller | | Reactive power internal controller | |
|---|---|---|---|---|---|---|---|---|
| | $K_{P1}$ (0.2–4) | $K_{I1}$ (0.2–4) | $K_{P2}$ (0.2–4) | $K_{I2}$ (0.2–4) | $K_{P3}$ (0.2–4) | $K_{I3}$ (0.2–4) | $K_{P4}$ (0.2–4) | $K_{I4}$ (0.2–4) |
| Mode 1 | Increasing damping | Decreasing damping | Increasing damping | Increasing damping | Increasing damping | Decreasing damping | Increasing damping until factor=2.4 and then decreasing damping | Increasing damping |
| Mode 3 | Increasing damping | Decreasing damping | Increasing damping | Decreasing damping | Decreasing damping | Increasing damping | Increasing damping until factor=2 and then decreasing damping | Decreasing damping |

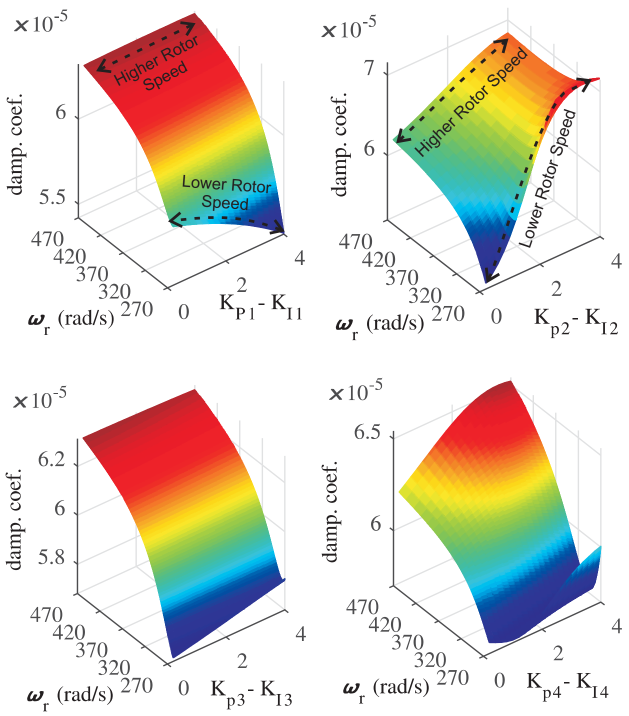


**Fig. 18:** Effect of rotor speed on the torsional interaction with DFIG active and reactive power controllers.

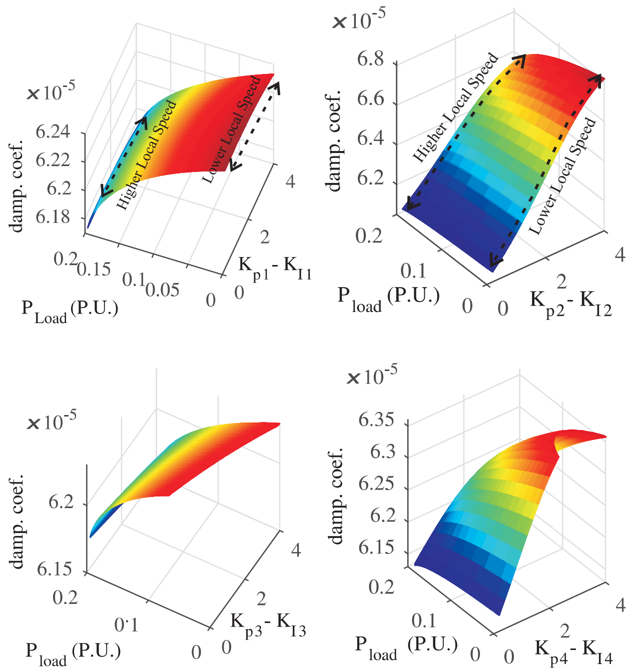


**Fig. 19:** Effect of local load on torsional interaction with DFIG active and reactive power controllers.

### 2) Local Load ($P_{Load}$)

In the test system, the local load is considered at bus A (Fig. 5). To study the effect of local load on the torsional interaction with DFIG controllers, the local load is increased from 0 to 0.2 pu and the results are shown in Fig. 19. The results show that, at lower local load, by increasing the gains active power controller ($K_{P1}$ and $K_{I1}$), the damping of torsional mode 1 is decreased, while at higher local load, by increasing the gains $K_{P1}$ and $K_{I1}$, the damping of torsional mode 1 is increased.

### 3) The Ratio of Turbine Inertia to the Generator Inertia ($H_{tur} \cdot (H_{gen})^{-1}$)

To investigate the effects of inertia of shaft sections on the torsional interaction with active and reactive power controllers, different values for inertia of shaft sections are considered. In this section, the turbine inertia is considered equal to total inertia of the turbine blades and the hub. By increasing the turbine inertia with respect to generator inertia from 1 to 10, as seen in Fig. 20, the damping of torsional modes is significantly decreased. But the effect of the active and reactive power controller is not different for various inertia ratios.

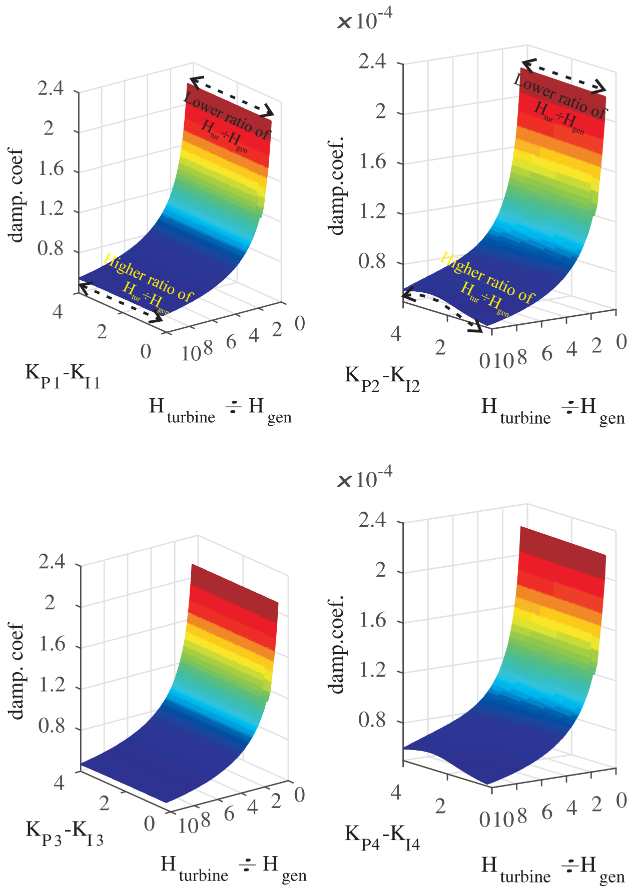


**Fig. 20:** Effect of shaft section inertia on the torsional interaction with DFIG active and reactive power controllers.

### 4) The Stator and Rotor Resistance and Reactance ($R_s$, $R_r$, $X_{Ls}$, $X_{Lr}$)

In this section for four electrical parameters of DFIG ($R_s$, $R_r$, $X_{Ls}$ and $X_{Lr}$), the torsional interaction of the wind turbine generator with DFIG active and reactive power controllers is investigated, and the results are shown in Fig. 21, Fig. 22, Fig. 23 and Fig. 24. The obtained results show that the electrical parameters of DFIG, especially the reactance of stator and rotor has significant effect on the torsional interaction with active and reactive power controllers. For instance, as seen in Fig. 23, at the lower DFIG stator reactance, by increasing the gains of active power internal controller ($K_{P2}$ and $K_{I2}$) and reactive power internal controller ($K_{P4}$ and $K_{I4}$), the damping of torsional mode 1 is slightly increased. While that at the higher DFIG stator reactance, by increasing the gains $K_{P2}$, $K_{I2}$, $K_{P4}$ and $K_{I4}$, the damping of torsional mode 1 is significantly decreased. In addition, the same results are obtained for DFIG rotor reactance (see Fig. 24).

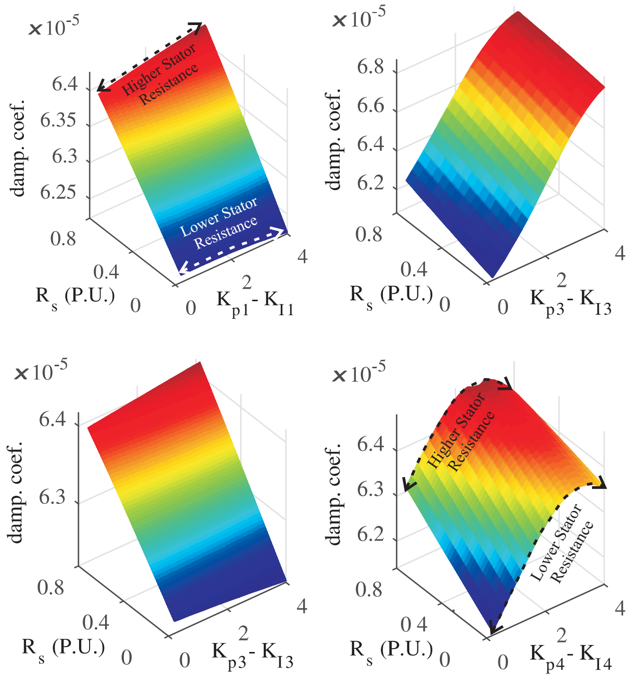


**Fig. 21:** Effect of DFIG stator impedance on torsional interaction with DFIG active and reactive power controllers.

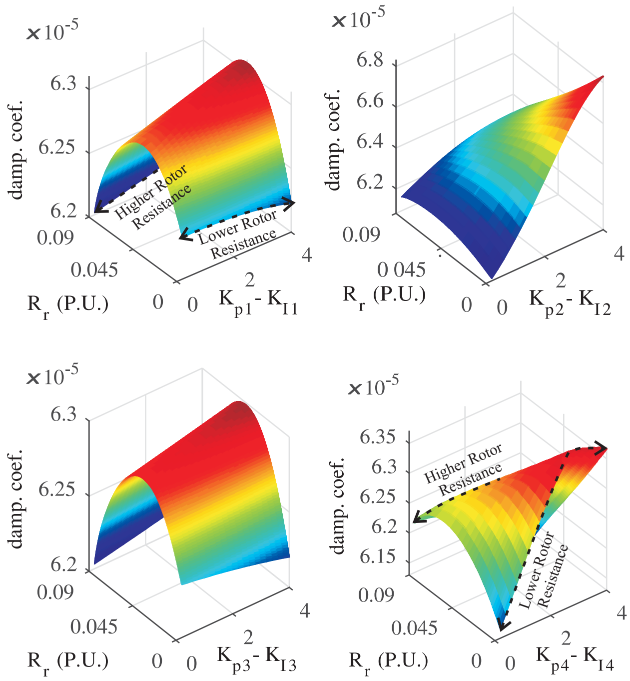


**Fig. 22:** Effect of DFIG rotor impedance on torsional interaction with DFIG active and reactive power controllers.

## 5. Conclusion

The wind energy utilization increased rapidly in recent years and it is now the most important source of electricity because of its availability and abundance in

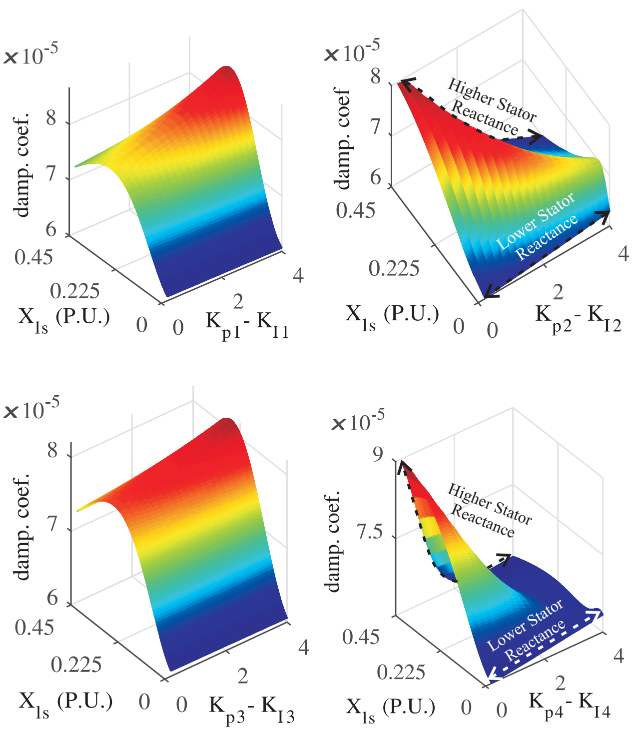


**Fig. 23:** Effect of DFIG stator reactance on torsional interaction with DFIG active and reactive power controllers.

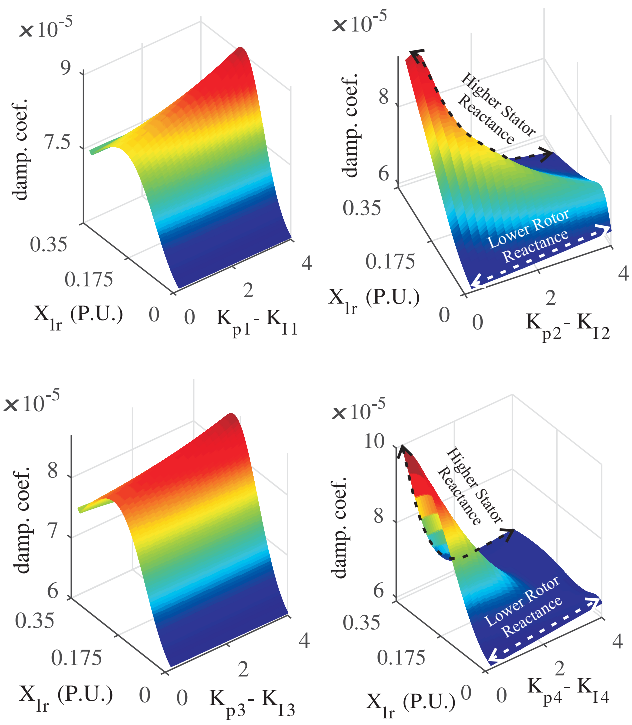


**Fig. 24:** Effect of DFIG rotor reactance on torsional interaction with DFIG active and reactive power controllers.

many places. The DFIG is the most promising generator in wind turbine applications due to the various advantages, such as the capability of independent control of active and reactive power, and power factor control. In order to ensure the performance of the wind turbine-generators, the interaction of the DFIG controllers with other components of the power system should be studied carefully. Therefore, in this paper, the interaction phenomenon was studied using the linear modal analysis. The important role of DFIG controller parameters in the occurrence of interaction with torsional modes of turbine-generator set was examined. Furthermore, the effects of some other factors, such as rotor speed, local load and shaft stiffness, on the damping ratio of torsional modes were also studied. The obtained results show that the DFIG controllers should be tuned properly; otherwise, the interaction may occur and the system oscillations increase, and in the worst case the system becomes unstable. The results show that the interaction of DFIG controllers will occur with both electrical and mechanical system modes leading to electrical and mechanical oscillations. However, the mechanical ones are more dangerous, since they have adverse effects on the lifetime of the turbine generator shaft.

Based on the present study the following can be remarked:

- The effect of the active power controller on the damping of torsional modes is more than that of reactive power. In addition, the effect of the external controllers is less than the internal controllers in both active and reactive ones.
- The rotor speed, local load and electrical parameters of DFIG can affect the torsional interaction between turbine generator shaft and DFIG controllers.
- Among the electrical parameters, the effect of DFIG stator and rotor reactance is severe than other parameters.

# References

[1] LI, H. and Z. CHEN. Transient Stability Analysis of Wind Turbines with Induction Generators Considering Blades and Shaft Flexibility. In: *33rd Annual Conference of the IEEE Industrial Electronics Society IECON 2007*. Taipei: IEEE, 2007, pp. 1604–1609. ISBN 1-4244-0783-4. DOI: 10.1109/IECON.2007.4460348.

[2] MUYEEN, S. M., M. HASAN ALI, R. TAKAHASHI, T. MURATA, J. TAMURA, Y. TOMAKI, A. SAKAHARA and E. SASANO. Transient Stability Analysis of Wind Generator System with the Consideration of Multi-Mass Shaft Model. In: *International Conference on*

*Power Electronics and Drives Systems*. Kuala Lumpur: IEEE, 2005, pp. 511–516. ISBN 0-7803-9296-5. DOI: 10.1109/PEDS.2005.1619740.

[3] WALKER, D. N., C. E. J. BOWLER, R. L. JACKSON and D. A. HODGES. Results of subsynchronous resonance test at Mohave. *IEEE Transactions on Power Apparatus and Systems*. 1975, vol. 94, iss. 5, pp. 1878–1889. ISSN 0018-9510. DOI: 10.1109/T-PAS.1975.32034.

[4] ZHU, C., L. FAN and M. HU. Control and analysis of DFIG-based wind turbines in a series compensated network for SSR damping. In: *IEEE PES General Meeting*. Michigan: IEEE, 2010, pp. 1–6. ISBN 978-1-4244-6549-1. DOI: 10.1109/PES.2010.5590091.

[5] SURIYAARACHCHI, D. H. R., U. D. ANNAKKAGE, C. KARAWITA and D. A. JACOBSON. A Procedure to Study Sub-Synchronous Interactions in Wind Integrated Power Systems. *IEEE Transactions on Power Systems*. 2013, vol. 28, iss. 1, pp. 377–384. ISSN 0885-8950. DOI: 10.1109/TPWRS.2012.2204283.

[6] MIAO, Z. Impedance-Model-Based SSR Analysis for Type 3 Wind Generator and Series-Compensated Network. *IEEE Transactions on Energy Conversion*. 2012, vol. 27, iss. 4, pp. 984–991. ISSN 0885-8969. DOI: 10.1109/TEC.2012.2211019.

[7] CHOWDHURY, M. A. and M. A. MAHMUD. Mitigation of subsynchronous control interaction in series-compensated DFIG-based wind farms using a nonlinear partial feedback linearizing controller. In: *IEEE Innovative Smart Grid Technologies - Asia (ISGT-Asia)*. Melbourne: IEEE, 2016, pp. 335–340. ISBN 978-1-5090-4303-3. DOI: 10.1109/ISGT-Asia.2016.7796408.

[8] LEE, D. C. and P. KUNDUR. Advanced Excitation Controls for Power System Stability Enhancement. *CIGRE* [online]. 1986, paper 38-01. Available at: e-cigre.org/publication/38-01_1986-advanced-excitation-controls-for-power-system-stability-enhancement–.

[9] LEE, D. C., R. E. BEAULIEU and G. J. ROGERS. Effects of Governor Characteristics on Turbo-Generator Shaft Torsionals. *IEEE Transactions on Power Apparatus and Systems*. 1985, vol. PAS-104, iss. 6, pp. 1254–1261. ISSN 0018-9510. DOI: 10.1109/TPAS.1985.319237.

[10] BAHRMAN, M., E. V. LARSEN, R. J. PIWKO and H. S. PATEL. Experience with HVDC - Turbine-Generator Torsional Interaction at Square Butte. *IEEE Transactions on Power Apparatus and Systems*. 1980, vol. PAS-99, iss. 3, pp. 966–975. ISSN 0018-9510. DOI: 10.1109/TPAS.1980.319726.

[11] CHOO, Y. C., A. P. AGALGAONKAR, K. M. MUTTAQI, S. PERERA and M. NEGNEVITSKY. Subsynchronous torsional interaction behaviour of wind turbine-generator unit connected to an HVDC system. In: *IECON 2010 - 36th Annual Conference on IEEE Industrial Electronics Society*. Glendale: IEEE, 2010, pp. 996–1002. ISBN 978-1-4244-5225-5. DOI: 10.1109/IECON.2010.5675504.

[12] HARNEFORS, L. Analysis of Subsynchronous Torsional Interaction With Power Electronic Converters. *IEEE Transactions on Power Systems*. 2007, vol. 22, iss. 1, pp. 305–313. ISSN 0885-8950. DOI: 10.1109/TPWRS.2006.889038.

[13] TOHIDI, S., A. RABIEE and M. PARNIANI. Influence of model simplifications and parameters on dynamic performance of grid connected fixed speed wind turbines. In: *The XIX International Conference on Electrical Machines - ICEM 2010*. Rome: IEEE, 2010, pp. 1–7. ISBN 978-1-4244-4174-7. DOI: 10.1109/ICELMACH.2010.5607919.

[14] SANCHEZ-GASCA, J. J., N. W. MILLER and W. W. PRICE. A modal analysis of a two-area system with significant wind power penetration. In: *IEEE PES Power Systems Conference and Exposition, 2004*. New York: IEEE, 2004, pp. 1537–1541. ISBN 0-7803-8718-X. DOI: 10.1109/PSCE.2004.1397695.

[15] RANJBAR, A. M. and M. JAFARIAN. Interaction of the dynamics of doubly fed wind generators with power system electromechanical oscillations. *IET Renewable Power Generation*. 2013, vol. 7, iss. 2, pp. 89–97. ISSN 1752-1416. DOI: 10.1049/iet-rpg.2012.0138.

[16] CHOO, Y. C., A. P. AGALGAONKAR, K. M. MUTTAQI, S. PERERA and M. NEGNEVITSKY. Analysis of Subsynchronous Torsional Interaction of HVDC System Integrated Hydro Units With Small Generator-to-Turbine Inertia Ratios. *IEEE Transactions on Power Systems*. 2014, vol. 29, iss. 3, pp. 1064–1076. ISSN 0885-8950. DOI: 10.1109/TPWRS.2013.2292857.

[17] FAN, L., C. ZHU, Z. MIAO and M. HU. Modal Analysis of a DFIG-Based Wind Farm Interfaced With a Series Compensated Network. *IEEE Transactions on Energy Conversion*. 2011, vol. 26, iss. 4, pp. 1010–1020. ISSN 0885-8969. DOI: 10.1109/TEC.2012.2160995.

[18] ALAWASA, K. M. and Y. A.-R. I. MOHAMED. A Simple Approach to Damp SSR in Series-Compensated Systems via Reshaping the Output Admittance of A Nearby VSC-based System. *IEEE Transactions on Industrial Electronics*. 2015, vol. 62, iss. 5, pp. 2673–2682. ISSN 0278-0046. DOI: 10.1109/TIE.2014.2363622.

[19] VAN, T. L., T. D. NGYEN, T. T. TRAN and H. D. NGUYEN. Advanced Control Strategy of Back-to-Back PWM Converters in PMSG Wind Power System. *Advances in Electrical and Electronic Engineering*. 2015, vol. 13, iss. 2, pp. 81–95. ISSN 1804-3119. DOI: 10.15598/aeee.v13i2.1161.

[20] LEON, A. E. and J. A. SOLSONA. Sub-Synchronous Interaction Damping Control for DFIG Wind Turbines. *IEEE Transactions on Power Systems*. 2015, vol. 30, iss. 1, pp. 419–428. ISSN 0885-8950. DOI: 10.1109/TPWRS.2014.2327197.

[21] STUCHLY, J., S. MISAK and L. PROKOP. A Simulation of Energy Storage System for Improving the Power System Stability with Grid-Connected PV using MCA Analysis and LabVIEW Tool. *Advances in Electrical and Electronic Engineering*. 2015, vol. 13, iss. 2, pp. 127–136. ISSN 1804-3119. DOI: 10.15598/aeee.v13i2.1347.

[22] ALI, M. T., M. GHANDHARI and L. HARNEFORS. Effect of control parameters on infliction of sub-synchronous control interaction in DFIGs. In: *2016 IEEE International Conference on Power and Renewable Energy (ICPRE)*. Shanghai: IEEE, 2016, pp. 72–78. ISBN 978-1-5090-3068-2. DOI: 10.1109/ICPRE.2016.7871175.

[23] PULGAR-PAINEMAL, H. A. *Wind Farm Model for Power System Stability Analysis*. Champaign, 2010. Dissertation thesis. University of Illinoise. Supervisor: P. W. Sauer.

[24] AGRAWAL, J. and S. BODKHE. Experimental Study of Low Speed Sensorless Control of PMSM Drive Using High Frequency Signal Injection. *Advances in Electrical and Electronic Engineering*. 2016, vol. 14, iss. 1, pp. 29–39. ISSN 1804-3119. DOI: 10.15598/aeee.v14i1.1564.

[25] YAZDANI, A. and R. IRAVANI. *Voltage-sourced converters in power systems: modeling, control, and applications*. Hoboken: John Wiley, 2010. ISBN 978-0-470-52156-4.

[26] AKHMATOV, V. An Aggregated Model of A Large Wind Farm With Variable Speed Wind Turbines Equipped With Doubly-Fed Induction Generators. *Wind Engineering*. 2004, vol. 28, iss. 4, pp. 479-486. ISSN 2048-402X. DOI: 10.1260/0309524042886423.

# About Authors

**Ali ZIAEI** was born in Zanjan, Iran. He received his B.Sc. and M.Sc. Degrees in electrical engineering from Ferdowsi University of Mashhad, Mashhad, Iran, in 2008 and 2012 respectively. His research interests include application of power electronics in power systems, power system dynamics, renewable energy, and wind power plants.

**Reza GHAZI** was born in Semnan, Iran. He received his B.Sc., degree (with honors) from Tehran University of Science and Technology, Tehran, Iran in 1976. In 1986, he received his M.Sc. degree from Manchester University, Institute of Science and Technology (UMIST) and the Ph.D. degree in 1989 from University of Salford UK, all in electrical engineering. He is currently professor of electrical engineering in Ferdowsi University of Mashhad, Mashhad, Iran. His main research interests are reactive power control, FACTS devices, power systems control, and analysis. He has published over 100 papers in these fields including three books.

**Roohalamin ZEINALI DAVARANI** was born in Rafsanjan, Iran. He received the B.Sc. degree from Shahid Bahonar University of Kerman, Kerman, Iran, in 2004. He obtained the M.Sc. and Ph.D. degrees from Ferdowsi University of Mashhad, Mashhad, Iran, respectively in 2007 and 2012, all in electrical engineering. He is currently assistant professor of electrical engineering in Graduate University of Advanced Technology, Kerman, Iran. His research interests include power system dynamic and control, renewable energies, and FACTS devices.

# Appendix A DFIG and Its Controllers Data

- $R_s = 0.023$ PU,
- $R_r = 0.016$ PU,
- $X_{ls} = 0.18$ PU,
- $X_{lr} = 0.16$ PU,
- $X_m = 2.9$ PU,
- $H_g = 0.54$ s,
- pole pair = 3,
- $V_n = 575$ V,
- $P_n = 1.5$ MW,
- $K_{P1} = K_{P3} = 0.05$,
- $K_{I1} = K_{I3} = 5$,

- $K_{P2} = K_{P4} = 0.3$,
- $K_{I2} = K_{I4} = 8$.

# Appendix B Wind Turbine Data

- $H_{blade} = 4.5$ s,
- $H_{hub} = 0.5$ s,
- $K_{bh} = 0.2$ PU,
- $K_{hg} = 1.6$ PU,
- $D_{bh} = 1.6$ PU,
- $D_{hg} = 1.5$ PU,
- $K_{gear} = 91$.